**EMISSION MEASUREMENTS OF LUNAR ANALOGUES FOR INTERPRETATION OF RETURNING DATA FROM THE DIVINER LUNAR RADIOMETER ON NASA'S LUNAR RECONNAISSANCE ORBITER.** I. R. Thomas[1], N. E. Bowles[1], B. T. Greenhagen[2], T. D. Glotch[3], K. L. Donaldson Hanna[4], M. B. Wyatt[4], J. L. Bandfield[5] and D. A. Paige[6], [1]Atmospheric, Oceanic and Planetary Physics Dept., University of Oxford, Oxford, UK (thomas@atm.ox.ac.uk), [2]Geophysics and Planetary Geosciences Group, Jet Propulsion Laboratory, Pasadena, CA, USA, [3]Dept. of Geosciences, Stony Brook University, Stony Brook, NY, USA, [4]Dept. of Geological Sciences, Brown University, Providence, RI, USA, [5]Dept. of Earth and Space Sciences, University of Washington, Seattle, WA, USA, [6]Dept. of Earth and Space Sciences, University of California, Los Angeles, CA, USA.

**Introduction:** Diviner (Instrument PI: David Paige, UCLA) is a nine-channel mapping radiometer currently orbiting the Moon onboard the Lunar Reconnaissance Orbiter. The instrument consists of two solar channels (0.35 – 2.8 μm), three '8 μm' channels (7.55 – 8.05, 8.1 – 8.4 and 8.4 – 8.7 μm) and four thermal channels (13 – 23, 25 – 41, 50 – 100, and 100 – 400 μm). Each channel contains 21 detectors, which from an orbit altitude of 50km allows a spatial resolution of less than 400 metres to be achieved [1]. These '8 μm' channels are specifically designed to map the spectral position of the Christiansen Feature (CF), in order to constrain lunar surface composition [2].

The CF is a mid-infrared emissivity maximum, which due to enhancement by the lunar environment is a prominent spectral feature observed in the mid-infrared (MIR) spectra of lunar minerals, and is also a good compositional indicator [2,3,4,5].

This enhancement is caused by a large thermal gradient being developed in the top few layers of the sample: During the lunar daytime, the solar diurnal temperature wave is capable of penetrating through the top few centimetres of regolith, heating it up, while the top few microns of the surface radiate to cold space and are therefore cooled. The very low thermal conductivity of the lunar regolith and lack of interstitial gases due to the very low pressure on the Moon, prevent efficient heat transport in the soil, setting up this strong thermal gradient. This appears in emission spectra as an enhanced emissivity peak, because in the region of the spectrum that is most transparent, radiation is emitted from hotter, deeper layers in the surface, as has been shown in previous studies [4,5,6,7,8].

**The Lunar Thermal Environment Simulator:** A new emission chamber was built to simulate the temperatures and pressures experienced on the lunar surface (figures 1 and 2). Modeling has shown [8] that these conditions can be replicated by heating a sample from below to 500K, whilst the sample is surrounded by a radiation shield cooled to 100-150K; all under a pressure of less than $10^{-6}$ bar. The cooled radiation shield is painted with very high emissivity paint, emulating cold space. The temperatures of the various parts are monitored by 6 PRTs, allowing accurate temperature control and some redundancy. The emission chamber is attached to the emission port of a Brüker IFS 66v Fourier Transform Spectrometer in the Atmospheric, Oceanic and Planetary Physics Dept. in Oxford. Heaters are attached to the off-axis paraboloid (OAP) mirror used to direct radiation from the sample into the spectrometer, allowing its temperature to be controlled independently of the cold shield. This prevents vapour given off by the sample from contaminating the mirror. For measurements, the OAP is cooled along with the radiation shield. Calibration of the spectrometer is achieved by making many regular high resolution measurements of a blackbody at known temperatures, as in [9], for example.

**Figure 1: A photo showing the lunar thermal environment simulator, spectrometer, vacuum pump and liquid nitrogen feed-throughs.**

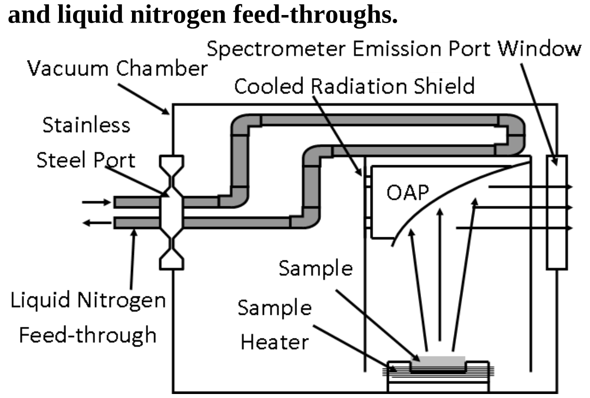


**Figure 2: A simplified diagram of the inside of the emission chamber, with the main parts labeled.**

**Minerals:** The lunar analogue minerals investigated were: albite, andesine, anorthite, augite, bytownite, diopside, enstatite, fayalite, forsterite, ilmenite, labradorite, oligoclase, quartz, and several mixtures consisting of these minerals in varying amounts. Each mineral was then separated into all or some of the following grain sizes distributions: 0 – 30, 30 – 64, 0 – 64, 64 – 120, and 120 – 450 microns, depending on quantity and structure of sample [10]. Timothy Glotch of Stony Brook University has also lent several obsidian and microcline samples, and Kerri Donaldson Hanna is planning to measure some samples loaned from Arizona State University in January 2010.

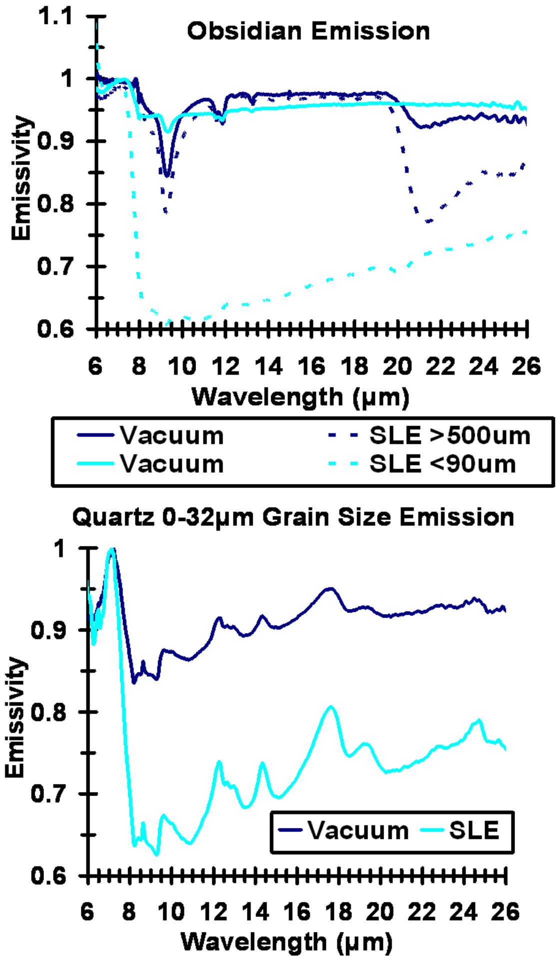


**Figure 3: Sample emission spectra of obsidian >500μm, obsidian <90μm, and quartz <32μm grain size distributions. The differences between measurements made under vacuum with an ambient radiation shield (labeled 'vacuum') and measurements in a SLE can clearly be seen.**

**Results:** Many expected trends have been observed in the spectra taken so far: 1) The location of the CF varies with mineral type; 2) the CF is enhanced in small grain size fractions by the simulated lunar environment (SLE), with reducing effect for increasingly large grain sizes; 3) the SLE causes the CF peak to shift to shorter wavelengths in some minerals, all agreeing with previously published data [5,6,7,8]. Some example spectra are shown in figure 3.

FIR emission can also be measured, by replacing the KBr window currently used with a polyethylene window. After sufficient spectra have been acquired, work will then begin on fitting these new spectra to the Diviner dataset.

**References:** [1] Paige D. A. et al. (2009) The Diviner Lunar Radiometer Experiment, Space Sci. Rev.; [2] Greenhagen B. T. (2009) Ph.D. Dissertation, UCLA; [3] Nash D. B. et al. (1993) J. Geophys. Res., 98, 23535-23552; [4] Logan L. M. et al. (1973) LPS III, 3069-3076; [5] Logan L. M. and Hunt G. R. (1970) Science, 169, 865-866; [6] Henderson & Jakosky (1997) J. Geophys. Res., 102, 6567-6580; [7] Logan et al. (1973) J. Geophys. Res., 78, 4983-5003; [8] Henderson et al. (1996) J. Geophys. Res., 101, 14969-14975; [9] Maturilli A. et al. (2006) Planet. Space Sci., 54, 1057-1064; [10] Greenhagen B. T. et al. (2008) EOS Trans. AGU, 89 (53), Fall Meet. Suppl.